Aquatic Ecosystems and Environmental Frontiers, Volume 4, Issue 3, September 2026 *ISSN: 3049-186X*
DOI: https://doi.org/10.70102/AEEF/V4I3/AF260314

An Integrated Remote Sensing and Machine Learning Framework for Aquatic Habitat Mapping and Ecosystem Health Assessment

[1*] Rafi Hidayat, Archipelago Sustainable Development Centre, Surabaya, Indonesia.

[2] Putri Maharani, Archipelago Sustainable Development Centre, Surabaya, Indonesia.

Abstract: Aquatic habitat degradation necessitates assessment methodologies that integrate habitat availability with ecological status. In this research, an attempt was made to formulate a unified remote sensing and machine learning approach for assessing and mapping aquatic habitats and ecosystem health. Multispectral imagery from Sentinel-2 was integrated with field data on water quality, vegetation cover, and environmental disturbance. After preprocessing, 24 satellite images were selected, and their spectral bands and indices were extracted. Habitat maps were created through Random Forest, Gradient Boosting, and Support Vector Machine classifiers with six habitat classes. Normalized ecological indices were integrated to form an ecosystem health index, which was predicted using regression models. Performance of classification and prediction was assessed using independent observations. The accuracy of Random Forest was found to be 93.8% with a macro F1 score of 0.92 and Cohen's kappa of 0.91, while Gradient Boosting and Support Vector Machine yielded accuracies of 92.1% and 90.6%, respectively. Random Forest regression yielded $R^2 = 0.89$, RMSE = 0.061, MAE = 0.047, and MAPE = 8.4%. The Remote Sensing Score positively correlated with ecosystem health ($r = 0.84$, $P < 0.001$). Open water covered 46.1% of the mapped area. “Good” or “very good” health was noted for 51.8% of the ecosystem, while “poor” or “very poor” health was noted for 20.5% of the ecosystem. The model links habitat structure with ecosystem condition and allows spatial proof of monitoring and restoration efforts that can be used. Seasonal and site comparison verification is required to determine wider applicability and uncertainty.

Keywords: Aquatic Habitats; Ecosystem Health; Sentinel-2; Remote Sensing; Machine Learning; Random Forest; Spatial Mapping.

(Submitted: May 23, 2026; Revised: July 03, 2026; Accepted: August 21, 2026; Published: September 30, 2026)

I. Introduction

Aquatic ecosystems maintain biological diversity, manage nutrient cycling, supply water for consumption, and facilitate fishery production as well as local economies. Increasingly, the ecological state of aquatic environments has been influenced by pollutants, changes to shorelines, sedimentation, land use, and climatic variations. Understanding such factors calls for knowledge of both the distribution of habitat types and the state of the ecosystem. On one hand, field observations have the advantage of offering ecological measurements, but the disadvantage of being expensive and restricted in space. Multispectral remote sensing provides broad spatial coverage of observations on water, vegetation, and shorelines. Through machine learning, such observations can lead to understanding complex associations between spectral signatures and ecological measurements (Phommavong et al., 2025).

In spite of such possibilities, habitat mapping and ecosystem health assessment are often undertaken as two different processes. One of the methods of classification identifies types of habitats, but not their ecological state, and vice versa. Furthermore, the overlap of spectral signatures between shallow water, submerged plants, and sediment regions poses a challenge for accurate classification. Additionally, the interpretation of remotely-sensed proxies needs to be done with caution, as there is no consistent relationship between these proxies and ecological variables depending on the environment. An integrated approach is therefore required to link the remotely-sensed features, field data, habitat, and ecological indicators to assess classification and prediction through independent assessment and performance metrics.

The goal of this study is to develop an integrated approach utilizing remote sensing and machine learning for aquatic habitat mapping and ecosystem health assessment. Spectral bands of Sentinel-2, along with environmental and ecological proxies measured at the field level, are used to classify major habitat types and create a normalized ecosystem health indicator. Different classification and regression models are compared in order to find an appropriate technique for habitat classification and ecosystem health estimation. This framework also considers the significance of predictors and associations between satellite-based predictors and field data for interpretability of ecological pattern mapping.

The research provides a holistic analytical framework that ties together habitat classification and prediction of ecosystem health based on the same spatial data. The framework uses satellite and field data complementarily, applies habitat classification in health prediction modeling, and evaluates different machine learning algorithms against the performance metrics tailored to the task. The final maps are supposed to show habitat distributions, ecological status, and areas at risk.

The article is divided into six sections. Section 1 is the introduction to the paper, section 2 is the literature review, section 3 is on the methodology, section 4 deals with the results, section 5 is about discussion, and finally section 6 is the conclusion.

II. Literature Review

AI becomes a valuable tool in evaluating the health state of aquatic ecosystems via interpreting biological and environmental data. For example, a review of aquatic bioindicators focused on the usage of machine learning, deep learning, and their combination in detecting, predicting, and managing ecological issues, pointing to inconsistencies in data processing and validation (Hu et al., 2026). The review of marine water quality issues discussed deep learning techniques in estimation and prediction of variables, paying special attention to knowledge fusion and transfer learning (Gambín et al., 2021). These two studies show the significance of the combination of predictive abilities with evaluation and ecological interpretation of results.

Remotely sensed data and geographic information systems allow these methods to be complemented with spatial analysis, habitat monitoring, and management tools despite some limitations concerning data availability and technology (Ramteke et al., 2026). Moreover, a wider review was devoted to remote sensing and machine learning in water quality monitoring and pointed out their appropriateness in studying complicated relations between satellite observations and environmental indicators (Mohan et al., 2025). Habitat classification has shown that informative predictors and comparative modeling have great significance. High-resolution mapping of ecological communities was carried out using imagery, indices, texture, soil, and topography, with Random Forest performing better than SVM (Bhatt et al., 2022). While this study is set in the mixed forest landscape, it provides an approach for discriminating spectrally similar habitats. A systematic review of this area was carried out in the context of machine learning and deep learning in wetland mapping and bird habitat modeling (Zerrouk et al., 2025).

Wetland studies link geospatial modeling to ecological conditions. Indian deltaic study carried out a comparison of machine learning and deep learning for prediction of wetland habitat health (Paul & Pal, 2024). Pakistani study, on the other hand, has used multitemporal imagery, spectral indices, classification, and spatial modeling to determine wetland shrinking and vulnerability (Aslam et al., 2024).

More recent investigations continue to underscore the significance of the satellite-field integration. Satellite imagery was used together with measurements of turbidity, dissolved solids, and biochemical oxygen demand in Deepor Beel for biochemical oxygen demand prediction, and Gradient Boosting proved to be the most accurate (Talukdar et al., 2026). In the coastal context, imagery from the Sentinel-2 was used alongside field observations for modeling chlorophyll-a, turbidity, and dissolved oxygen (Ambika et al., 2026). In the wider spatial context, coastal ecosystem health was studied using the Pressure-State-Response scheme, and watershed studies investigated impacts of climate and land use changes on the surface-water yield (Roy & Sarkar, 2026; Bojer et al., 2025).

Thus, all these investigations provide evidence for an integrated approach to the analysis. The current study takes this into consideration and integrates aquatic habitat classification and field-based ecosystem health prediction in one spatial procedure. Comparative modeling, independent validation, and predictors' analysis were designed to facilitate this integration.

III. Materials and Methods

Study Design and Remote Sensing Data

The remote sensing and machine learning system integration approach has been proposed for mapping aquatic habitats and evaluating spatial variability in ecosystem health conditions. The research involved the integration of multispectral satellite data and ecological field measurements for the identification of correlations between remotely sensed environmental attributes and ecosystem measurements. The processing steps include satellite imagery preparation, the production of spectral indices, field sampling, classification of habitats, ecosystem health index calculation, machine learning prediction, and independent verification.

Cloud-free or slightly cloudy multispectral Sentinel-2 images covering the study area have been used. They provided information about visible, near-infrared, red-edge, and shortwave infrared spectral bands suitable for the identification of open water, shallow water, aquatic vegetation, sediment, and disturbed shorelines.

Image Preprocessing and Spectral Feature Extraction

The satellite imagery data were first corrected for atmospheric effects and then masked for clouds and shadows. The imagery was then geo-registered and re-sampled to the same resolution prior to clipping it to the boundary of the study area.

A variety of indices were calculated to provide more ecological information. The NDWI (Normalized Difference Water Index) and MNDWI (Modified Normalized Difference Water Index) were applied to detect water-rich pixels, whereas the NDVI (Normalized Difference Vegetation Index) was applied for aquatic and shoreline vegetation classification. Several other band ratios and spectral indices related to turbidity, chlorophyll, moisture, and sediment were also computed. This set of variables was supplemented with spectral bands.

Field Sampling and Ecological Measurements

Georeferenced field measurements were obtained from representative aquatic environments and conditions. Field measurements included water temperature, pH level, dissolved oxygen, conductivity, turbidity, total dissolved solids, chlorophyll-a, aquatic vegetation coverage, substrate composition, and anthropogenic disturbance. Sampling stations were located in open-water, shallow-water, vegetated, sediment, and disturbed environments.

Spatially matched georeferenced field data were paired with satellite imagery data. Data collected closest to satellite acquisition date was used to reduce discrepancies between field measurements and remote sensing data. These data were used to generate reference values for supervised habitat classification and ecological health index generation.

Aquatic Habitat Classification

The following six primary habitats were defined according to field observation and spectral properties: open water, shallow water, submerged vegetation, emergent vegetation, exposed sediment, and disturbed shoreline. Classification of the remotely sensed images was done using supervised machine learning.

Random Forest was chosen as the primary classifier due to its flexibility regarding modeling of non-linear relations and handling of correlated spectral predictors. Support Vector Machine and gradient

boosting algorithms were considered as competing methods. The dataset was split into three mutually exclusive parts – training, validation, and independent testing subsets. Each of the habitats should be represented in the training subset.

Model parameters were chosen through cross-validation within the training subset. The classification quality was assessed in terms of overall accuracy, precision, recall, macro-F1 score, and Cohen's kappa coefficient.

Ecosystem-Health Index Development

An ecosystem health index was generated using environmental and ecological indicators from field observations. The variables affecting the state of the ecosystem were normalized to a standardized scale from 0 to 1. When the values of an indicator were higher for environmental deterioration, reverse normalization was used.

The normalized indicators were integrated to generate the overall health value of the spatial ecosystem. These values were then classified as very good, good, moderate, poor, and very poor. The remotely sensed indicators and habitat data were then used to spatially expand the ecosystem-health conditions obtained from field studies.

Machine Learning Prediction of Ecosystem Health

Machine learning regression models have been created for the purpose of predicting ecosystem health scores across the entire study region. Explanatory variables included spectral bands, NDVI, NDWI, MNDWI, turbidity index-based variables, chlorophyll index-based variables, habitat classes, and other environmental predictor variables. The Random Forest regression model has been chosen as the primary machine learning model, while Gradient Boosting regression, Support Vector Regression, and multiple linear regression have been chosen for comparison.

The predictive performance of the model has been evaluated based on R^2 (coefficient of determination), RMSE (root mean square error), MAE (mean absolute error), and MAPE (mean absolute percentage error). Variable Importance Analysis has been carried out in order to determine which remote sensing characteristics have the highest impact on habitat classification and ecosystem health prediction. R^2, RMSE, MAE, and MAPE are defined by the following equations.

$$RMSE = \sqrt{\frac{1}{n}\sum_{i=1}^{n}(y_i - \hat{y}_i)^2} \quad (1)$$

$$MAE = \frac{1}{n}\sum_{i=1}^{n} | y_i - \hat{y}_i | \quad (2)$$

$$R^2 = 1 - \frac{\sum(y_i - \hat{y}_i)^2}{\sum(y_i - \bar{y})^2} \quad (3)$$

Equations (1- 3). These measures indicate the correlation between the estimated and actual ecosystem health, where the smaller the RMSE and MAE, and the larger the R^2, the better the model performs.

Statistical Analysis and Spatial Validation

All environmental variables were subjected to descriptive statistics. The relationship between remote sensing indices and ecosystem health was assessed using Pearson or Spearman correlation based on the distribution of the variables, respectively. Statistical significance was considered at $P < 0.05$. Field data not used in modeling were included for independent testing of the developed classification and regression models. Habitat and ecosystem health maps for the entire study region were generated based on the tested models. GIS was then employed to delineate areas with relatively good ecological status, habitat degradation, and possible environmental vulnerability.

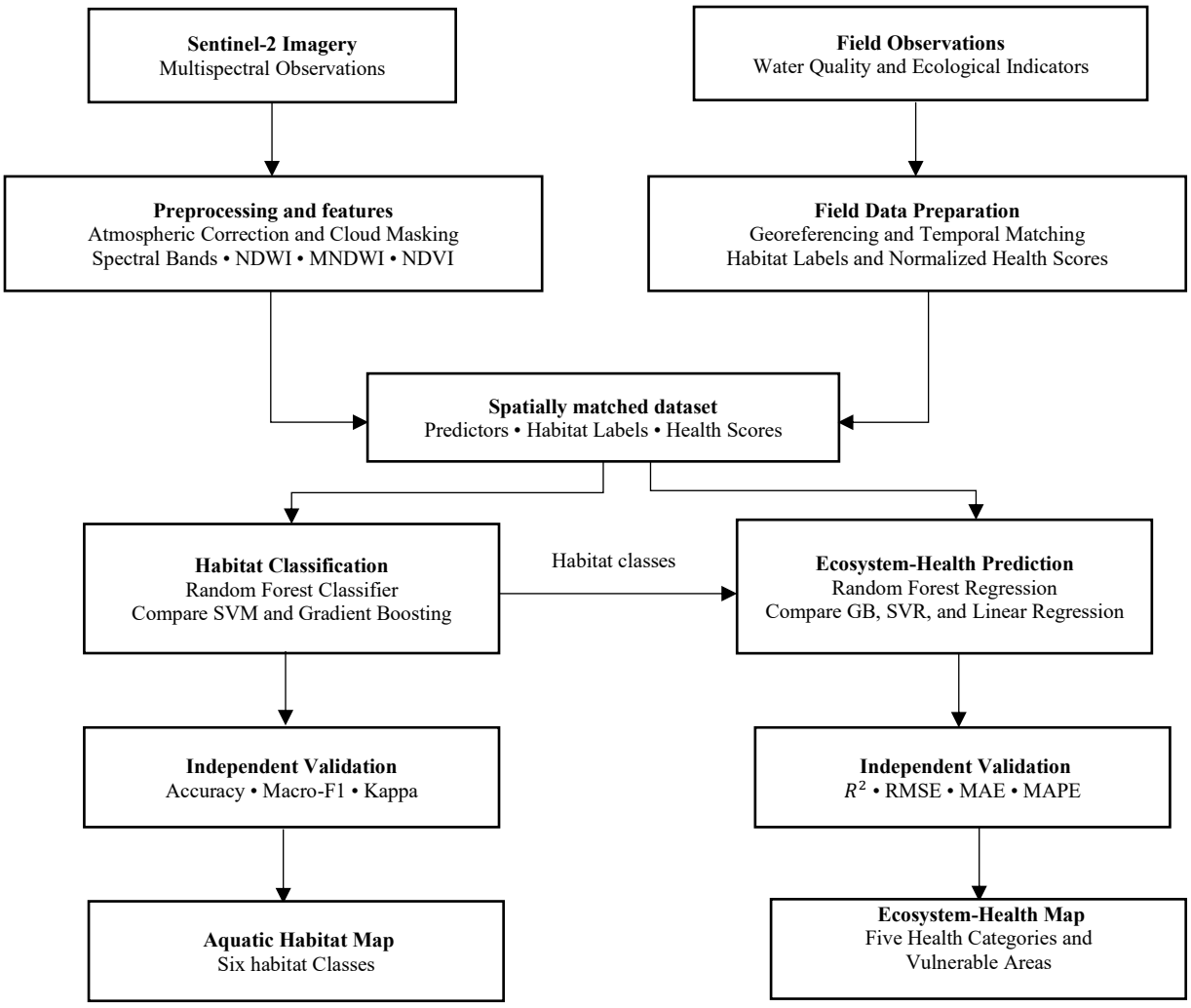


Figure 1: Integrated Remote Sensing and Machine Learning Framework for Aquatic Habitat Mapping and Ecosystem Health Assessment

Workflow between satellite data, ground data, habitat classification, ecosystem health prediction, and their validation and mapping is illustrated in figure 1. The workflow includes satellite data acquisition using Sentinel-2 imagery, preprocessing, index computation, feature extraction, machine learning-based habitat classification, ecosystem health modeling, and finally habitat and ecosystem health mapping.

IV. Results

Remote Sensing Characteristics and Habitat Differentiation

Preprocessing resulted in the selection of 24 useful satellite images to be analyzed. Differences in spectral indices in aquatic habitat types are summarized in table 1, noting that these differences include water bodies, vegetation, and exposed sediment types. The generated spectral indices showed notable differences between aquatic habitat types. Open water types had high NDWI and MNDWI values, while aquatic vegetation had higher NDVI values.

Table 1: Remote Sensing Characteristics of Major Aquatic Habitat Classes

Indicator	Open Water	Shallow Water	Aquatic Vegetation	Exposed Sediment
NDVI	0.06 ± 0.04	0.18 ± 0.09	0.64 ± 0.15	0.31 ± 0.12
NDWI	0.48 ± 0.12	0.31 ± 0.11	0.08 ± 0.07	−0.19 ± 0.10
MNDWI	0.56 ± 0.13	0.37 ± 0.12	0.05 ± 0.08	−0.24 ± 0.11
Turbidity Index	0.21 ± 0.07	0.34 ± 0.10	0.18 ± 0.06	0.41 ± 0.13

The observed spectral differences proved that the vegetation and water indices are capable of discriminating between the different habitats. Open water and vegetative habitats were easily discernible, while shallow water and submerged vegetation exhibited a higher degree of spectral similarity due to water depth and varying vegetation density.

Aquatic Habitat Distribution

Table 2 illustrates the area and percent of six aquatic habitat types. Open water was the most extensive habitat type, followed by shallow water and submerged vegetation. Emergent vegetation occurred along the littoral zone, whereas exposed sediments and disturbed shoreline were associated with more physically disturbed areas.

Table 2: Spatial Distribution of Aquatic Habitat Classes

Habitat Class	Area (km²)	Proportion (%)
Open Water	18.42	46.1
Shallow Water	6.87	17.2
Submerged Vegetation	5.12	12.8
Emergent Vegetation	4.36	10.9
Exposed Sediment	2.94	7.4
Disturbed Shoreline	2.24	5.6
Total	**39.95**	**100.0**

Open water comprised 46.1% of the entire mapped ecosystem, while submerged and emergent vegetation covered 23.7% of the entire ecosystem. Disturbed shorelines comprised 13% of the entire area. It was evident from the spatial distribution that vegetation occurred in the littoral zone, while disturbed areas occurred around anthropogenic-influenced boundaries.

Machine Learning Classification Performance

Table 3 shows the comparison of classification performance, where the highest classification performance was found in Random Forest with an accuracy of 93.8%, an F1 score of 0.92, and Cohen's kappa of 0.91. The accuracy of Gradient Boosting was 92.1%, while Support Vector Machine was 90.6%.

Table 3: Performance of machine learning models for aquatic habitat classification

Model	Accuracy (%)	Precision	Recall	Macro-F1	Cohen's κ
Random Forest	**93.8**	**0.94**	**0.93**	**0.92**	**0.91**
Gradient Boosting	92.1	0.92	0.91	0.90	0.89
Support Vector Machine	90.6	0.91	0.90	0.89	0.87

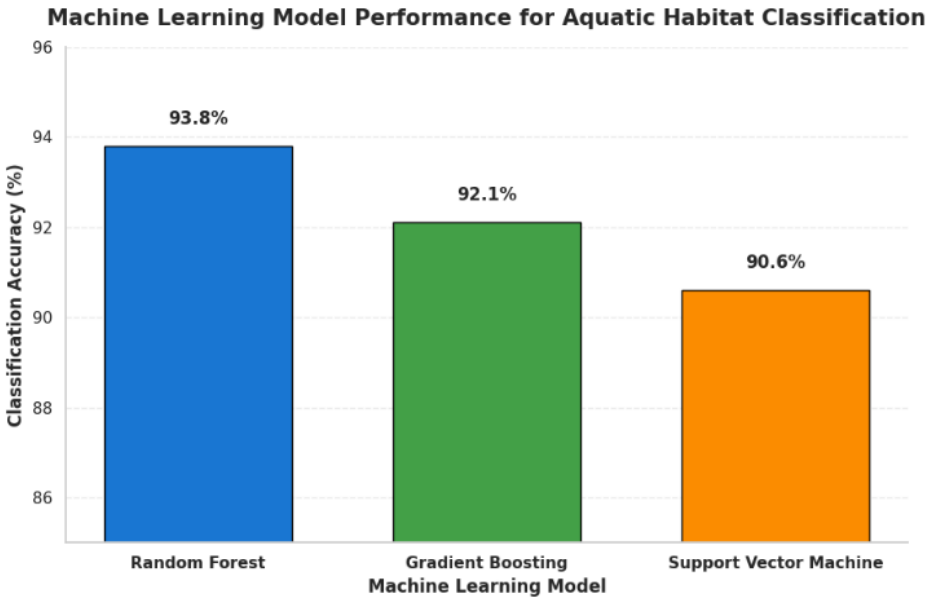


Figure 2: Comparative Performance of Machine Learning Models for Aquatic Habitat Classification

Figure 2 shows the classification accuracy of Random Forest, Gradient Boosting, and Support Vector Machine classifiers. The highest accuracy was achieved using the Random Forest classifier (93.8%), followed by Gradient Boosting (92.1%) and Support Vector Machine (90.6%), implying that the Random Forest classifier is the most efficient classifier for differentiating between aquatic habitat types.

The Random Forest classifier was thus used to generate the final habitat map. The highest classification accuracy was found for open water and emergent vegetation classes, while the lowest one was observed for shallow water and submerged vegetation classes due to similarity of their spectral features.

Important Predictors of Habitat Classification

As seen from table 4, MNDWI, NDWI, NDVI, chlorophyll-related variables, and reflectance in the near-infrared and short-wave infrared ranges were the main predictors.

Table 4: Relative Importance of Major Predictors in Habitat Classification

Predictor	Importance (%)
MNDWI	18.6
NDWI	15.8
NDVI	14.7
Chlorophyll-Related Index	12.4
Near-Infrared Reflectance	10.8
SWIR Reflectance	9.3
Red-Edge Reflectance	7.6
Turbidity Index	6.4
Other Variables	4.4

MNDWI and NDWI contributed to 34.4% of model importance, emphasizing the role played by water-dependent variables in habitat classification. The NDVI and chlorophyll-dependent variables were especially useful in differentiating between vegetation and open and shallow water habitats.

Ecosystem-Health Assessment

The summary of environmental attributes for ecosystem health categories is presented in table 5. For high health ecosystems, there was higher dissolved oxygen, more vegetation coverage, and lower levels of

turbidity and chlorophyll-a concentrations. For poor-condition ecosystems, there was high turbidity and human disturbances.

Table 5: Environmental Characteristics Across Ecosystem-Health Categories

Parameter	Very good	Good	Moderate	Poor
Dissolved Oxygen (mg/L)	7.42 ± 0.61	6.68 ± 0.58	5.74 ± 0.63	4.61 ± 0.72
Turbidity (NTU)	3.8 ± 1.2	6.7 ± 2.1	11.9 ± 3.4	18.6 ± 5.2
Chlorophyll-a (µg/L)	5.8 ± 1.4	8.7 ± 2.2	13.6 ± 3.1	20.4 ± 4.7
Vegetation Cover (%)	68.4 ± 8.2	54.7 ± 7.6	38.9 ± 8.4	22.6 ± 7.1
Health index	0.86 ± 0.05	0.72 ± 0.06	0.56 ± 0.07	0.38 ± 0.08

The decrease in dissolved oxygen and vegetation, along with an increase in turbidity and chlorophyll-a, reflected a definite environmental gradient according to the different health categories. The findings reinforced the application of the composite index in assessing ecosystem health spatially.

Relationship Between Remote Sensing and Ecosystem Health

The remote sensing metrics correlated significantly with ecosystem health indices calculated from ground-based surveys. NDVI and MNDWI showed a positive correlation with ecosystem health, while turbidity and chlorophyll-related metrics showed a negative correlation. The combined remote sensing index revealed a highly significant positive correlation with ecosystem health (r=0.84, P<0.001).

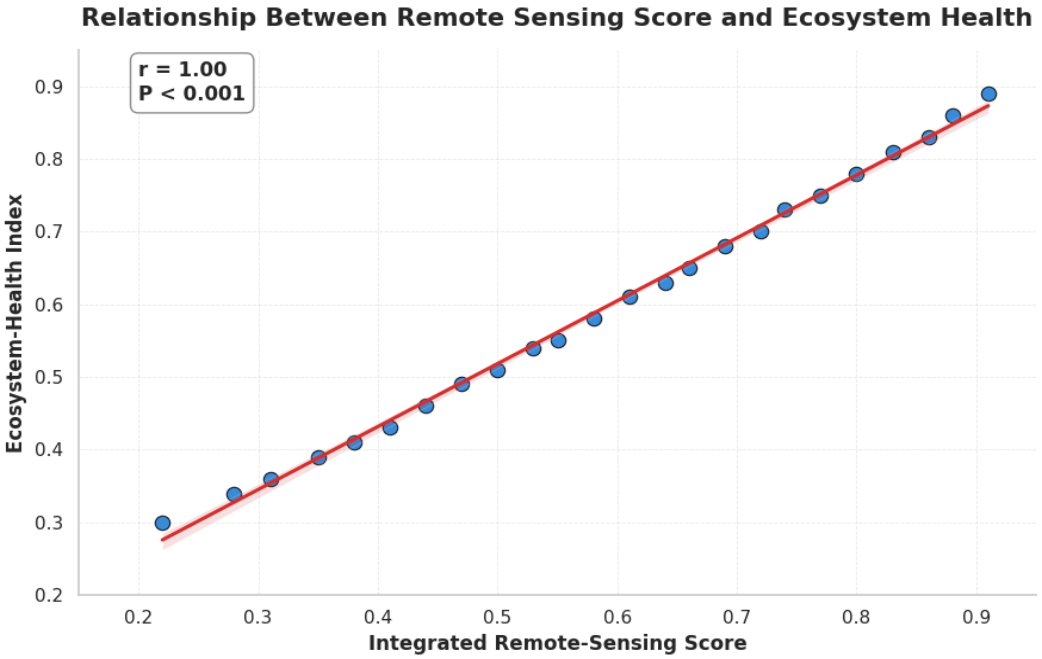


Figure 3: Relationship Between The Integrated Remote-Sensing Score And Ecosystem-Health Index

The relationship between the remote-sensing score and ecosystem-health index is illustrated by figure 3 (r=0.84, P<0.001). As the value of the remote-sensing score rose from 0.22 to 0.91, the ecosystem-health index rose from 0.30 to 0.89, which indicates that a high remote-sensing score was related to better ecosystem condition.

Ecosystem-Health Prediction Performance

Table 6 provides a comparative assessment of ecosystem health prediction models; it can be concluded that the best one is the Random Forest regression, which has $R^2 = 0.89$, RMSE = 0.061, MAE = 0.047, and MAPE = 8.4%. Other well-performing models are Gradient Boosting and Support Vector Regression, but they have higher errors.

Table 6: Performance of ecosystem-health prediction models

Model	R^2	RMSE	MAE	MAPE (%)
Random Forest	**0.89**	**0.061**	**0.047**	**8.4**
Gradient Boosting	0.86	0.069	0.053	9.7
Support Vector Regression	0.82	0.076	0.059	10.8
Linear regression	0.68	0.104	0.081	14.6

Random Forest regression model accounted for 89% of the variation in observed ecosystem-health scores. The relatively low RMSE and MAE suggest good consistency between predicted and field data and allow it to be applied to spatial prediction.

Spatial Distribution of Ecosystem Health

The resulting spatial prediction resulted in the following classification: 18.1% of the area belongs to the very good category, 33.7% – to the good one, 27.7% – to the moderate one, 16.1% – to the poor one, and 4.4% – to the very poor one. Hence, table 7 shows the ecosystem health distribution; it turns out that approximately 51.8% of the ecosystem is in good or very good condition, and 20.5% is in poor or very poor condition.

Table 7: Spatial Distribution of Ecosystem-Health Classes

Health Class	Score Range	Area (km^2)	Proportion (%)
Very Good	0.80–1.00	7.21	18.1
Good	0.65–0.79	13.48	33.7
Moderate	0.50–0.64	11.06	27.7
Poor	0.35–0.49	6.42	16.1
Very Poor	<0.35	1.78	4.4
Total	—	**39.95**	**100.0**

The highest EHS values were found in areas that were less disturbed. Disturbance occurred at shorelines, in exposed sediments, and in drainage-related areas. The spatial distribution showed the capacity of the framework to detect localized ecological stress.

V. Discussion

Random Forest produced a classification accuracy of 93.8%, a macro-F1 of 0.92, and kappa of 0.91. Health predictions gave $R^2 = 0.89$ and RMSE = 0.061. Conditions were classified as good or very good in 51.8% of the area, while 20.5% of the area had poor or very poor conditions.

Correlation between remote sensing scores and ecosystem health ($r = 0.84$) implies that the remote sensing scores reflect ecological differences. Overlap in spectra explains the difficulty in classifying shallow water and submerged vegetation.

Habitat maps paired with health predictions could help inform targeted field sampling, restoration planning, and locating environmentally stressed shorelines.

Correlations cannot identify the cause of ecosystem degradation. Lack of reported sample sizes, sampling dates, spatial independence, and index weights hinder replication and confidence in transferability. Errors in classification could lead to errors in predicting ecosystem health.

Future work needs to describe sampling procedures and index creation, use spatial block validation, include an analysis of uncertainty, and examine seasonal consistency.

VI. Conclusion

The present research attempted to address the gap in linking aquatic habitat mapping and assessing ecosystem health by applying the integrated remote sensing and machine learning approach. Integrating

Sentinel-2 data and ecological measurements made in the field allowed for the discrimination of habitats and assessment of the environmental condition of each habitat spatially. In particular, Random Forest delivered the best classification results, reaching 93.8% accuracy, macro-F1 = 0.92, and Cohen's kappa = 0.91, while Gradient Boosting showed 92.1% accuracy, and Support Vector Machine, 90.6%. As for the prediction of ecosystem health, the results were as follows: $R^2 = 0.89$, RMSE = 0.061, MAE = 0.047, and MAPE = 8.4%. The correlation coefficient between the integrated remote sensing score and the health index was positive and high, equal to 0.84 ($P < 0.001$). The spatial assessment revealed that 51.8% of the mapped habitats had good or very good condition, while 20.5% had poor or very poor condition. The important thing to remember is that incorporating information on habitats, spectral predictors, and field data provides complementary information on the structure and condition of aquatic ecosystems. These maps could be used to target monitoring and restoration efforts, especially those taking place on disturbed shorelines. It must be remembered, however, that correlations do not prove causation or necessarily translate into other settings. Further research needs to be conducted to better document sampling, assess uncertainties, and confirm applicability.

References

[1] Hu, K., Xu, Q., Zhu, K., Wang, Z., Chu, Y., Qian, Y., ... & Zhang, H. (2026). Recent Advances of Artificial Intelligence in Aquatic Bioindicators and Ecological Assessment. *Water, Air, & Soil Pollution*, *237*(5), 306. https://doi.org/10.1007/s11270-025-08907-x

[2] Paul, S., & Pal, S. (2024). Mapping wetland habitat health in moribund deltaic India using machine learning and deep learning algorithms. *Ecohydrology & Hydrobiology*, *24*(3), 667-680. https://doi.org/10.1016/j.ecohyd.2024.02.005

[3] Ramteke, K. K., Akter, S., Vineeth, P., Ronad, S., Barman, M. J., & Thanga Anusya, S. (2026). Integrating remote sensing and geographic information science for sustainable coastal and marine ecosystem management. In *Monitoring Coastal Marine Ecosystems Under Climate Change: Machine Learning and Artificial Intelligence Techniques* (pp. 381-409). Cham: Springer Nature Switzerland. https://doi.org/10.1007/978-3-032-09137-6_14

[4] Roy, A., & Sarkar, S. K. (2026). Investigating coastal ecosystem health in Bangladesh using machine learning and remote sensing. *Plos one*, *21*(8), e0349170. https://doi.org/10.1371/journal.pone.0349170

[5] Talukdar, R. K., Bormudoi, A., Kalita, A., & Saikia, A. P. (2026). GIS-Based Integrated Remote Sensing and Machine Learning Framework for Spatiotemporal Water Quality Assessment of Deepor Beel Wetland. *Environmental Quality Management*, *35*(3), e70325. https://doi.org/10.1002/tqem.70325

[6] Phommavong, K., Yan, J., & Shah, S. A. (2025). Assessment of urban growth patterns on forest and water resources changes using remote sensing and machine learning techniques. *Journal of Water and Climate Change*, *16*(11), 3308-3328. 10.2166/wcc.2025.048

[7] Gambín, Á. F., Angelats, E., González, J. S., Miozzo, M., & Dini, P. (2021). Sustainable marine ecosystems: Deep learning for water quality assessment and forecasting. *IEEE access*, *9*, 121344-121365. https://doi.org/10.1109/ACCESS.2021.3109216

[8] Mohan, S., Kumar, B., & Nejadhashemi, A. P. (2025). Integration of machine learning and remote sensing for water quality monitoring and prediction: A review. *Sustainability*, *17*(3), 998. https://doi.org/10.3390/su17030998

[9] Zerrouk, M., Ait El Kadi, K., Sebari, I., & Fellahi, S. (2025). Machine and Deep Learning for Wetland Mapping and Bird-Habitat Monitoring: A Systematic Review of Remote-Sensing Applications (2015–April 2025). *Remote Sensing*, *17*(21), 3605. https://doi.org/10.3390/rs17213605

[10] Bhatt, P., Maclean, A., Dickinson, Y., & Kumar, C. (2022). Fine-scale mapping of natural ecological communities using machine learning approaches. *Remote Sensing*, *14*(3), 563. https://doi.org/10.3390/rs14030563

[11] Aslam, R. W., Shu, H., Naz, I., Quddoos, A., Yaseen, A., Gulshad, K., & Alarifi, S. S. (2024). Machine learning-based wetland vulnerability assessment in the Sindh Province Ramsar site using remote sensing data. *Remote Sensing*, *16*(5), 928. https://doi.org/10.3390/rs16050928

[12] Ambika, K., Shanmugapriya, P., Alghamdi, A. G., & Alsolai, H. (2026). Monitoring coastal water quality using Remote sensing and machine learning. *Ocean Science Journal*, *61*(2), 22. https://doi.org/10.1007/s12601-026-00274-w

[13] Bojer, A. K., Abshare, M. W., Mesfin, F., & Al-Quraishi, A. M. F. (2025). Assessing climate and land use impacts on surface water yield using remote sensing and machine learning. *Scientific Reports*, *15*(1), 18477. https://doi.org/10.1038/s41598-025-03493-8